

A Proposal for Detecting Superfluidity in Neutron Stars

Yunjing Gao,¹ Jiahao Yang,¹ Zhenyu Zhu,¹ Yosuke Mizuno,^{1,2,*} and Jianda Wu^{1,2,†}

¹*Tsung-Dao Lee Institute, Shanghai Jiao Tong University, Shanghai 201210, China*

²*School of Physics and Astronomy, Shanghai Jiao Tong University, Shanghai 200240, China*

(Dated: October 20, 2022)

Based on the GW dispersion relation raised in [1], we investigate the possible reflection of gravitational wave (GW) by superfluidity (SF) in the neutron star, provided its high density and dissipationless properties. Following this scenario, an experimental proposal is raised to probe the expected SF in neutron star by means of GW detection. Two types of binary systems are considered, neutron star-black hole and binary neutron star systems, with weak gravitational field condition imposed. Non-negligible modulation on the total signal caused by the GW reflection is found, which contributes amplitude and phase variations distinguishable from the primitive sine signal. Furthermore, we show that it is possible for such modulations to be detected by the Cosmic Explorer and Einstein Telescope at 100 Mpc. Identification of those signals can evince the existence of the long-sought SF in neutron stars as well as the exotic superfluidity-induced GW reflection.

Introduction.— Superfluidity (SF) in neutron star (NS) has been predicted and discussed for a long time [2, 3]. Given high stellar density in NS, roughly $10^{14}g/cm^3$, the neutron pairing is expected to take place in the crust as well as outer core since its critical temperature ($\sim 10^{10}K$) is much larger than the typical temperature of NSs except for the formation stage [2, 4, 5]. In addition, for the charged particles, superconductivity of protons is possible at the crust-core interface, with the critical temperature on the same scale as neutron pairing [6]. In contrast, pairing of compressed electrons in NS is excluded, due to its exponentially small critical temperature $T_c \approx 3 \times 10^3 \rho_e^{1/6} e^{-2.8\rho_e^{1/3}} K$ with the electron density $\rho_e \sim 10^{12}g/cm^3$ [4]. Continuous efforts have been devoted to verifying SF in NS. One possible evidence comes from the observation of glitch (e.g., [7]), and a widely accepted explanation attributes such phenomenon to release of pinned vorticity of the neutron SF, which leads to angular momentum transfer in NS [8]. From another point of view, Ref. [9] shows that the cooling procedure of the Cassiopeia A Neutron Star is 4% faster than conventional prediction [10] during the last ten years, whose cooling mechanism can be explained by enhanced neutrino emission during pairing formation of neutrons [11].

The observations of GW170817 [12], GW200105 and GW200115 [13] capture the emission of GW in a binary neutron star (BNS) system and neutron star-black hole (NSBH) systems, providing a possibility to connect the detection of SF in NS to GW observation. From the GW dispersion relation raised in the study of GW interaction with fermionic SF [1], the contribution can be divided into “diamagnetic” and “paramagnetic” parts. A similar mechanism has also been pointed out in [14]. The absorption for GW is described by the imaginary part of the paramagnetic term, which corresponds to the quasi-particle excitation in the SF discussed here. Competition between the “diamagnetic” and “paramagnetic” terms can lead to different propagation scenarios of GW, including a regime where the GW will be reflected.

If the reflection from NS can happen, it will give rise to a modulation for the observed GW signals. In return, a direct observation of the modulation can provide one-stone-two-bird evidence: 1, it supports the existence of SF in NS; 2, it implies the GW reflection from SF. In this letter, first we show an estimation on the possible GW reflection by SF in the NS, corresponding to typical GW frequency measurable nowadays. Based on this feature, we study the modulation signal caused by reflection from two systems: the NSBH system and the BNS system. The modulation signal contributes non-negligible amplitude and phase deviations, whose variation with GW frequency and mass of the NS (or black hole) is studied. Furthermore, we show that the modulation can possibly be probed by the Cosmic Explorer as well as Einstein Telescope in a reasonable parameter region.

Mechanism for GW reflection.— The response of superfluidity to incident GW can be described by the GW dispersion relation [1]

$$\omega_{\text{GW}}^2 \approx c^2 k_{\text{GW}}^2 + \frac{32\pi GP}{c^2} + \frac{16\pi G\chi}{c^2}, \quad (1)$$

where P stands for the pressure in SF and χ is the response function of stress-energy tensor variation to the metric perturbation. The second term on the right hand side serves as a “diamagnetic” term to the GW, which comes from the metric dependency of stress-energy tensor. The third term referred to as “paramagnetic” term has a non-local nature, which originates from the variation of SF density matrix with respect to the metric [14], and can be described by the linear response theory [15]. Since the energy scale of typical NS temperature is much smaller than the pairing gap, the results derived by the zero temperature formalism is a reasonable approximation for the cases here.

Given the degeneracy pressure about 1.6×10^{34} Pa in the NSs [16], the diamagnetic part dominates the dispersion. Simple calculation tells us that when $\omega_{\text{GW}} \lesssim \omega_{\text{cut}} \approx 3 \times 10^4$ Hz the GW has a purely imaginary wave vector

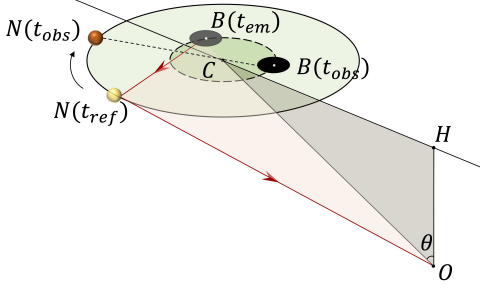


FIG. 1. Illustration for GW reflection in the NSBH system. Here N , B , C and O stand for NS, BH, rotation center and observer, respectively. θ denotes the inclination angular of observer. Plane CHO is perpendicular to the orbital plane which crosses the perigee. The red lines and arrows track the reflection signal propagation. In the local time of observer, the orange-shaded ball illustrates real-time position for the NS, and the reflection signal received at this time comes from $N(t_{ref})$ (yellow-shaded ball) at some earlier time, which is emitted at $B(t_{em})$ by the BH.

resulting in a finite penetration depth correspondingly. Moreover, for typical GW, as observed in real detections, its frequency is much smaller than ω_{cut} , as such the penetration depth is approximately 8.6×10^3 m which is a few times smaller than the NS diameter. Furthermore, within the zero temperature approximation, $\text{Im}[\chi] = 0$ as typical GW frequency $\omega_{GW} \ll 2\Delta/\hbar$ (Δ is the pairing gap). The vanishing imaginary part indicates no absorption of GW energy by the SF, combined with the finite penetration depth, significant reflection of GW is expected in the dense and dissipationless superfluid layer of NSs.

The NSBH system. — The total signal (E_{tot}) consists of direct incident (E_{dir}) and reflection (E_{ref}) parts. For E_{dir} , quadrupole moment approximation is applied to determine the amplitude, which considers the NS and black hole (BH) as a whole contributor. Both NS and BH are assumed to rotate around the mass center C in a circular motion without eccentricity. The propagation distance before observation is taken as $|CO|$, and $|\cdot|$ stands for the distance between two points. By taking Newtonian orbital approximation, the orbital radius $R_{orb} = (GM_{BH}/\omega_\alpha^2)^{1/3}$, where the angular velocity $\omega_\alpha = \omega_{GW}/2$, and G is the gravitational constant. For direct signal received at t_{obs}

$$E_{dir}(t_{obs}) = \frac{\mathcal{E}_0^{dir}}{|CO|} e^{-i\phi_0(t_{obs})}, \quad (2)$$

where $\mathcal{E}_0^{dir} = 4GR_{orb}^2 M_{NS} \omega_\alpha^2 / c^4$, $\phi_0(t) = \omega_{GW} t - k_{GW}|CO|$ with k_{GW} being the GW wave vector and c being the speed of light.

For the reflection part, the GW on the surface of NS is assumed to be fully reflected for simplicity, as the NS radius is larger than the penetration depth. Due to the complexity of GW emission from the source and the

reflection mechanism, a phenomenological model is employed to simplify this process. Contribution from BH to the GW is extracted as a result of quadrupole moment variation of BH rotating around the center of mass (C in Fig. 1). This part of GW propagates outward spherically from $B(t_{em})$ and is reflected on the surface of NS at a later time t_{ref} with amplitude $\mathcal{E}_0^{ref}/|B(t_{em})N(t_{ref})| = 4GR_{BH}^2 M_{BH} \omega_\alpha^2 / (c^4 |B(t_{em})N(t_{ref})|)$, where $R_{(\cdot)}$ stands for orbital radius. The NS plays the role of “spherical mirror” of GW. Since the typical radius of NSs ($r_{NS} \approx 20$ km) is much smaller than the wavelength of GW of interest, isotropic reflection is considered. After being scattered by the NS, amplitude of the outgoing GW which propagates to the observer O at time t_{obs} becomes $(\mathcal{E}_0^{ref}/|ON(t_{ref})|) \cdot (r_{NS}/|B(t_{em})N(t_{ref})|)$.

Distances between NS and BH located at different times have been encountered here, which can be determined by finding the propagation time relation. Both t_{em} and t_{ref} are referred to as functions of t_{obs} , whose relations are shown in [17]. In the following, we denote the propagation distance before and after reflection corresponding to GW observed at t_{obs} as $L_b(t_{obs}) = c(t_{ref} - t_{em})$ and $L_a(t_{obs}) = c(t_{obs} - t_{ref})$. As a result, the reflection signal can be formally given by

$$E_{ref}(t_{obs}) = \frac{\mathcal{E}_0^{ref} r_{NS} e^{-i[\omega_{GW} t_{obs} - k_{GW}(L_a(t_{obs}) + L_b(t_{obs}))]}}{L_a(t_{obs}) L_b(t_{obs})} \quad (3)$$

As a simple example, in the limit $k(R_{BH} + R_{NS}) \ll 1$, t_{em} can be treated as a constant shift of t_{ref} . Also, since $|CO| \gg R_{BH}$, the reflection signal can be simplified as

$$E_{ref}^{lim}(t_{obs}) = \frac{\mathcal{E}_0^{ref} r_{NS} e^{-i[\phi_0(t_{obs}) + \kappa \cos[\omega_\alpha(t_{obs} - |CO|/c)]}}{|CO| R_{BH} + R_{NS}}, \quad (4)$$

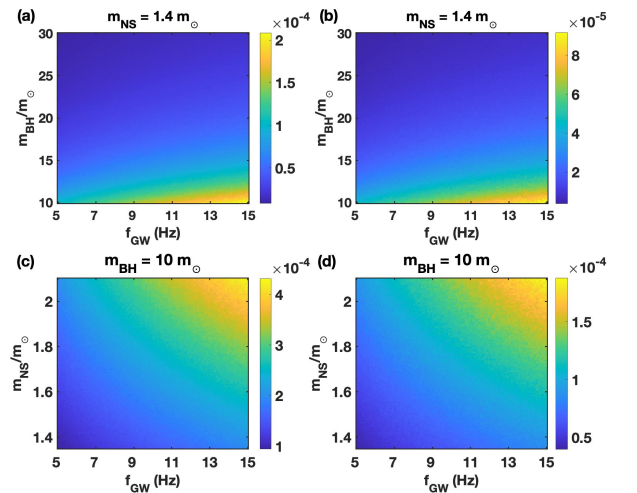


FIG. 2. Plot of σ_A in (a, c) and σ_ϕ in (b, d) for the NSBH system with $\theta = \pi/2$. The first row is fixed for $m_{NS} = 1.4 m_\odot$ and the second row with fixed $m_{BH} = 10 m_\odot$.

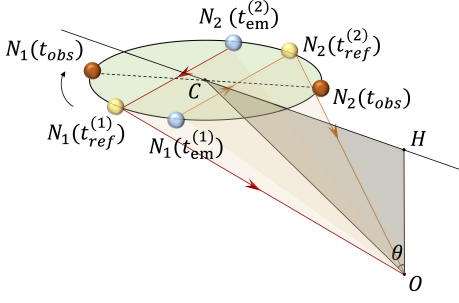


FIG. 3. Illustration for GW reflection in the BNS system. C, H, O, θ , *ibid.*(Fig. 1). The orange and red arrows and lines show the paths of reflection signals. Two orange-shaded balls label the real-time positions of the two NSs. Yellow-shaded balls are the positions of NSs when reflection happens, each related to one blue-shaded ball denoting the emission position.

with $\kappa = k_{\text{GW}} R_{\text{NS}} \sin \theta$. The contribution of reflection signal can be seen clearly if we consider the Fourier component of Eq.(4). Apart from the dominant contribution at $f_{\text{GW}} = \omega_{\text{GW}}/2\pi$, additional components at $f_{\text{GW}}/2, 3f_{\text{GW}}/2, 2f_{\text{GW}}, \dots$ show up. This can be viewed from the expansion of $\exp[i\kappa \cos(\omega_{\alpha} t_{\text{obs}})]$, where $\kappa^n \cos^n(\omega_{\alpha} t_{\text{obs}})$ can be rewritten as a summation of $\kappa^n \exp[\pm im(\omega_{\alpha} t_{\text{obs}})]$ terms with $m, n \in N$. The additional peaks lead to distinct difference in the observation result.

In the general case, E_{tot} can be expressed in a compact form after combining Eq. (2) and Eq. (3), and we define $\gamma(t) = (\mathcal{E}_0^{\text{ref}}/\mathcal{E}_0^{\text{dir}})(r_{\text{NS}}/L_b(t))$. Since it is sufficient to consider the properties of one GW component, then

$$\text{Re}[E_{\text{tot}}(t_{\text{obs}})] = \frac{\mathcal{E}_0}{|CO|} \mathcal{A}(t_{\text{obs}}) \cos[\phi_0(t_{\text{obs}}) - \phi(t_{\text{obs}})], \quad (5)$$

where

$$\mathcal{A}(t) = \sqrt{1 + \gamma^2(t) + 2\gamma(t) \cos[k_{\text{GW}}(L_b(t) + L_a(t) - |CO|)]}$$

$$\tan \phi(t) = \frac{\gamma(t) \sin[k_{\text{GW}}(L_b(t) + L_a(t) - |CO|)]}{1 + \gamma(t) \cos[k_{\text{GW}}(L_b(t) + L_a(t) - |CO|)]}. \quad (6)$$

As a consequence of E_{ref} , the explicit modulations appear in the relative amplitude $\mathcal{A}(t)$ and the non-linear phase $\phi(t)$ of $\text{Re}[E_{\text{tot}}]$. Both modulations are at the same order of magnitude of γ , whose effect can be viewed from the standard deviations of the two quantities,

$$\sigma_{\mathcal{A}} = \sqrt{\langle \mathcal{A}^2 \rangle - \langle \mathcal{A} \rangle^2}$$

$$\sigma_{\phi} = \sqrt{\langle \phi^2 \rangle - \langle \phi \rangle^2}, \quad (7)$$

where $\langle \cdot \rangle = \int_0^{T_{\text{orb}}} \cdot dt / T_{\text{orb}}$ with T_{orb} being the orbital period. As can be observed from Eq. (6), more significant fluctuations occur for larger γ and k_{GW} . Moreover, $\gamma \propto M_{\text{NS}} M_{\text{BH}}^{1/3} / (M_{\text{BH}} + M_{\text{NS}})^{5/3}$ approximately. This is consistent with the result of $\sigma_{\mathcal{A}}$ and σ_{ϕ} shown in Fig. 2.

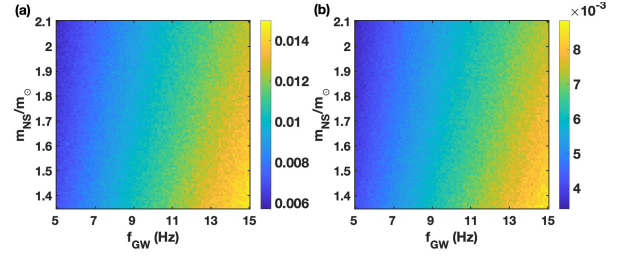


FIG. 4. Plot for $\sigma_{\mathcal{A}}$ (a) and σ_{ϕ} (b) in the BNS system with $\theta = \pi/2$.

Larger M_{NS} leads to stronger fluctuations for both $\sigma_{\mathcal{A}}$ and σ_{ϕ} , while it is opposite for M_{BH} . As f_{GW} gets larger, the fluctuations are significantly enhanced.

The BNS system.— As in the NSBH case the same treatment is applied in this system. Two NSs, N_1 and N_2 in Fig. 3, are assumed to have equal mass. Then the direct incident signal generated by the whole system take the form

$$\tilde{E}_{\text{dir}} = \frac{\tilde{\mathcal{E}}_0^{\text{dir}}}{|CO|} e^{-i\tilde{\phi}_0(t_{\text{obs}})}, \quad (8)$$

with $\tilde{\phi}_0(t_{\text{obs}}) = \omega_{\text{GW}} t_{\text{obs}} - k_{\text{GW}} |CO|$ and $\tilde{\mathcal{E}}_0^{\text{dir}} = 8\pi G \tilde{R}_{\text{NS}}^2 M_{\text{NS}} \omega_{\alpha}^2 / c^4$ with the orbital radius $\tilde{R}_{\text{NS}} = (GM_{\text{NS}}/4\omega_{\alpha}^2)^{1/3}$. We use $\tilde{E}_{\text{ref}}^{(\cdot)}$ and $L_{a(b)}^{(\cdot)}$ to represent reflection signal and propagation distance before (b) and after (a) the reflection happens, which is related to reflection on $N_{(\cdot)}$. Then the reflection signal is given by

$$\tilde{E}_{\text{ref}}(t_{\text{obs}}) = \tilde{E}_{\text{ref}}^{(1)}(t_{\text{obs}}) + \tilde{E}_{\text{ref}}^{(2)}(t_{\text{obs}})$$

$$= \frac{\tilde{\mathcal{E}}_0^{\text{ref}}}{L_a^{(1)}(t_{\text{obs}}) L_b^{(1)}(t_{\text{obs}})} \frac{r_{\text{NS}}}{e^{-i[\omega_{\text{GW}} t_{\text{obs}} - k_{\text{GW}}(L_a^{(1)}(t_{\text{obs}}) + L_b^{(1)}(t_{\text{obs}})])}}$$

$$+ \frac{\tilde{\mathcal{E}}_0^{\text{ref}}}{L_a^{(2)}(t_{\text{obs}}) L_b^{(2)}(t_{\text{obs}})} \frac{r_{\text{NS}}}{e^{-i[\omega_{\text{GW}} t_{\text{obs}} - k_{\text{GW}}(L_a^{(2)}(t_{\text{obs}}) + L_b^{(2)}(t_{\text{obs}})])}}, \quad (9)$$

where $\tilde{\mathcal{E}}_0^{\text{ref}} = 4G \tilde{R}_{\text{orb}}^2 M_{\text{NS}} \omega_{\alpha}^2 / c^4$ and the distance relations can be found in [18]. In the limit $k_{\text{GW}} R_{\text{NS}} \ll 1$, t_{ref} can be treated as a constant shift of t_{obs} , leading to the approximation result

$$\tilde{E}_{\text{ref}}^{\text{lim}}(t_{\text{obs}}) = \frac{\tilde{\mathcal{E}}_0^{\text{ref}}}{|CO|} \frac{r_{\text{NS}}}{|2R_{\text{NS}}|} e^{i(\omega_{\text{GW}} t_{\text{obs}} - 2k_{\text{GW}} R_{\text{NS}})}$$

$$\times 2 \cos(\kappa \cos[\omega_{\alpha}(t_{\text{obs}} - |CO|/c)]). \quad (10)$$

Frequency components in addition to f_{GW} appear as can be observed by expanding $\cos(\kappa \cos(\omega_{\alpha}(t_{\text{obs}})))$ in the small κ , whose values take $0, 2f_{\text{GW}}, 3f_{\text{GW}}, \dots$.

In the observation, the two branches of reflection signal superimpose on the direct incident part, giving rise to the following result for real part of the total signal

$$\text{Re}[\tilde{E}_{\text{tot}}(t_{\text{obs}})] = \frac{\tilde{\mathcal{E}}_0^{\text{dir}}}{|CO|} \tilde{\mathcal{A}}(t_{\text{obs}}) \cos[\tilde{\phi}_0(t_{\text{obs}}) - \tilde{\phi}(t_{\text{obs}})], \quad (11)$$

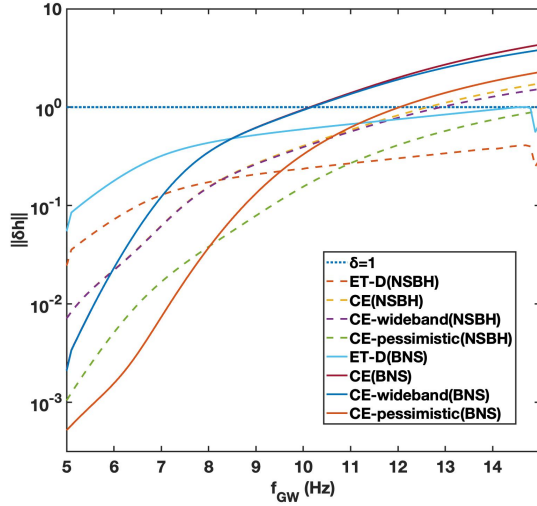


FIG. 5. Plot of $\|\delta h\|$ at 100 Mpc with the Cosmic Explorer and Einstein Telescope for NSBH and BNS systems. The bold blue line plots $\|\delta h\| = 1$ as a reference.

where

$$\begin{aligned} \tilde{\mathcal{A}}(t) = & \left(1 + 2\tilde{\gamma}(t)(\cos\tilde{\phi}^{(1)} + \cos\tilde{\phi}^{(2)}) \right. \\ & \left. + \tilde{\gamma}(t)^2 [2 + 2\sin\tilde{\phi}^{(1)}\sin\tilde{\phi}^{(2)} + 2\cos\tilde{\phi}^{(1)}\cos\tilde{\phi}^{(2)}] \right)^{\frac{1}{2}} \end{aligned} \quad (12)$$

and

$$\tan\tilde{\phi}(t) = \frac{\sin\tilde{\phi}^{(1)} + \sin\tilde{\phi}^{(2)}}{1 + \tilde{\gamma}(t)(\cos\tilde{\phi}^{(1)} + \cos\tilde{\phi}^{(2)})}, \quad (13)$$

with

$$\begin{aligned} \tilde{\phi}^{(1)} &= \sin[k_{\text{GW}}(L_a^{(1)}(t) + L_b^{(1)}(t) - |CO|)] \\ \tilde{\phi}^{(2)} &= \sin[k_{\text{GW}}(L_a^{(2)}(t) + L_b^{(2)}(t) - |CO|)]. \end{aligned} \quad (14)$$

The relative amplitude $\tilde{\mathcal{A}}(t)$ and non-linear phase $\tilde{\phi}(t)$ in $\text{Re}[E_{tot}]$ show explicit modulation in the presence of \tilde{E}_{ref} . Standard deviation $\sigma_{\tilde{\mathcal{A}}}$ and $\sigma_{\tilde{\phi}}$ can be defined in the same way as Eq. (7). Also, the modulations in $\tilde{\mathcal{A}}(t)$ and $\tilde{\phi}(t)$ are at the order of $\tilde{\gamma}$, which is approximately proportional to $M_{\text{NS}}^{-1/3}$. As a result, both $\sigma_{\tilde{\mathcal{A}}}$ and $\sigma_{\tilde{\phi}}$ exhibit increasing tendencies with larger f_{GW} but smaller M_{NS} as is shown in Fig. 4. Those non-negligible fluctuations cause distinguishable modifications compared with the non-reflection model.

Signal distinguishability.— In this section we estimate the practical ability for the modulated signal caused by GW reflection to be distinguishable in GW detection. As the discussion in [19], two waveforms h_1 and h_2 are distinguishable in principle if

$$\|\delta h\| \equiv \sqrt{\langle h_1 - h_2 | h_1 - h_2 \rangle} \gtrsim 1 \quad (15)$$

is satisfied, where the noise-weighted inner product is given by

$$\langle h_1 - h_2 | h_1 - h_2 \rangle = 4 \text{Re} \int_0^\infty \frac{|h_1(f) - h_2(f)|^2}{S(f)} df, \quad (16)$$

and $S(f)$ is the instrument noise spectrum. In the comparison of the reflection model with the non-reflection one, difference between two waveforms is given by E_{ref} (\tilde{E}_{ref}). Here we test the distinguishability of the reflection signal using several analysis model for Cosmic Explorer and Einstein Telescope [20–22]. In the following calculation, the distance $|CO| = 100$ Mpc, $M_{\text{BH}} = 10M_\odot$, $M_{\text{NS}} = 2M_\odot$ and $r_{\text{NS}} = 20$ km. An increasing tendency for $\|\delta h\|$ has been found as f_{GW} gets larger in the frequency region we are interested in. The modulation signal is experimentally distinguishable in principle for f_{GW} which gives $\|\delta h\| > 1$. Due to the larger NS rotational radius in BNS system compared with BH in NSBH case, more significant reflection signal should be expected from the former case, which can be consistently observed from Fig. 5 for each type of detector model. Furthermore, a wider observable region for the reflection signal is expected with more sensitive detectors in next generations.

Conclusion.— To conclude, we give an estimation to show the possible GW reflection by SF in the NSs, given the GW frequency in observable region. Based on this property, we demonstrate the possibility of detecting SF in NSs based on GW measurements. In both NSBH and BNS systems, reflected GW signals contribute non-negligibly to the total signal, and modulate the amplitude and phase term at the order of ratio of NS radius to orbital radius. The modulation is captured by the fluctuations of the amplitude and the linear phase, which increases with the angular velocity. Lastly, we show that such modulations caused by the GW reflection are detectable with Cosmic Explorer and Einstein Telescope in a reasonable parameter region. The observation results after comparison with our theoretical predictions can provide evidence to support the existence of SF as well as GW reflection of neutron stars.

Y. G., J. Y., and Z. Z. contribute equally to this study.

* mizuno@sjtu.edu.cn

† wujd@sjtu.edu.cn

- [1] A. Cetoli and C. J. Pethick, *Phys. Rev. D* **85**, 064036 (2012).
- [2] A. B. Migdal, *Nucl. Phys.* **13**, 655 (1959).
- [3] G. Baym, C. Pethick, and D. Pikes, *Nature* **224**, 674 (1969).
- [4] V. L. Ginzburg, *J. Stat. Phys.* **1**, 3 (1969).
- [5] R. A. Wolf, *Astrophys. J.* **145**, 834 (1966).
- [6] N. Chamel and P. Haensel, *Living Rev. Relativ.* **11**, 10 (2008).

- [7] R. N. Manchester and J. H. Taylor, *Astrophys. J.* **191**, L63 (1974).
- [8] P. W. Anderson, *Nature* **256**, 25 (1975).
- [9] C. O. Heinke and W. C. G. Ho, *Astrophys. J. Lett.* **719**, L167 (2010).
- [10] A. Y. Potekhin, G. Chabrier, and D. G. Yakovlev, *Astron. Astrophys.* **323**, 415 (1997), [arXiv:astro-ph/9706148](#).
- [11] D. Page, M. Prakash, J. M. Lattimer, and A. W. Steiner, *Phys. Rev. Lett.* **106**, 081101 (2011).
- [12] B. P. Abbott *et al.* (LIGO Scientific, Virgo Collaborations), *Phys. Rev. Lett.* **119**, 161101 (2017).
- [13] R. Abbott *et al.* (LIGO Scientific, Virgo, KAGRA Collaborations), *Astrophys. J. Lett.* **915**, L5 (2021).
- [14] Y. V. Gratz, *Sov. Phys. J.* **33**, 344 (1990).
- [15] J. W. Negele and H. Orland, *Quantum Many-particle Systems* (Westview Press, 1998).
- [16] F. Özel and P. Freire, *Annual Review of Astronomy and Astrophysics* **54**, 401 (2016).
- [17] The NS is initially set at the perigee, namely $\angle HCN(t) = \omega_\alpha t$. The distance relation is simply

$$|ON(t)| = \sqrt{|CO|^2 + R_{\text{NS}}^2 - 2R_{\text{BH}}|CH| \cos(\omega_\alpha t)}$$

$$|N(t)B(t - \Delta t)| = \sqrt{R_{\text{NS}}^2 + R_{\text{BH}}^2 + 2R_{\text{NS}}R_{\text{BH}} \cos(\omega_\alpha \Delta t)}, \quad (17)$$

with $R_{\text{BH}} = (G(M_{\text{NS}})^3 / (M_{\text{NS}} + M_{\text{BH}})^2 \omega_\alpha^2)^{1/3}$ and $R_{\text{NS}} = (G(M_{\text{BH}})^3 / (M_{\text{NS}} + M_{\text{BH}})^2 \omega_\alpha^2)^{1/3}$. GW signal received at t_{obs} is reflected by NS at a previous time t_{ref} , which comes from emission at time t_{em} . Subjecting to the GW propagation procedure we have

$$c(t_{\text{obs}} - t_{\text{ref}}) = \sqrt{|CO|^2 + R_{\text{NS}}^2 - 2R_{\text{BH}}|CH| \cos(\omega_\alpha t_{\text{ref}})}$$

$$c\Delta t = \sqrt{R_{\text{NS}}^2 + R_{\text{BH}}^2 + 2R_{\text{NS}}R_{\text{BH}} \cos(\omega_\alpha \Delta t)}, \quad (18)$$

with $\Delta t = t_{\text{ref}} - t_{\text{em}}$. By solving the set of equations numerically, we can find the propagation distance as well as the reflection amplitude and phase.

- [18] The propagation procedure is similar to the NSBH case, but with the NS being source and “mirror” simultaneously. The reflection time are determined independently for the two stars (denote with superscripts $(1)(2)$), namely

$$c(t_{\text{obs}} - t_{\text{ref}}^{(1)}) = \sqrt{|CO|^2 + R_{\text{NS}}^2 - 2|CH|R_{\text{NS}} \cos(\omega_\alpha t_{\text{ref}}^{(1)})},$$

$$c(t_{\text{obs}} - t_{\text{ref}}^{(2)}) = \sqrt{|CO|^2 + R_{\text{NS}}^2 + 2|CH|R_{\text{NS}} \cos(\omega_\alpha t_{\text{ref}}^{(2)})}. \quad (19)$$

And the time retardations (Δt) between emission and reflection are the same for both NSs, satisfying $c\Delta t = 2R_{\text{NS}} \cos(\omega_\alpha \Delta t/2)$.

- [19] J. S. Read, L. Baiotti, J. D. E. Creighton, J. L. Friedman, B. Giacomazzo, K. Kyutoku, C. Markakis, L. Rezzolla, M. Shibata, and K. Taniguchi, *Phys. Rev. D* **88**, 044042 (2013).
- [20] B. P. Abbott *et al.* (LIGO Scientific Collaboration), *Class. Quant. Grav.* **34**, 044001 (2017).
- [21] S. Hild *et al.*, *Class. Quant. Grav.* **27**, 015003 (2009).
- [22] S. Hild *et al.*, *Class. Quant. Grav.* **28**, 094013 (2011).